

## Simulations of point-defect properties in graphite by a tight-binding-force model

C. H. Xu, C. L. Fu, and D. F. Pedraza

*Metals and Ceramics Division, Oak Ridge National Laboratory, P.O. Box 2008, Oak Ridge, Tennessee 37831*

(Received 21 January 1993; revised manuscript received 21 June 1993)

Point-defect energetics and diffusion mechanisms in graphite are investigated using a semi-empirical tight-binding-force model. Possible diffusion processes associated with point-defect (i.e., vacancies and interstitials) and nondefect (i.e., atomic exchange) mechanisms are analyzed. It is found that self-diffusion in graphite in the direction parallel to the basal plane can be mediated by vacancies. However, since the calculated vacancy- and interstitial-formation energies are nearly equal, it is argued that Frenkel pairs could exist as equilibrium defects. In this case, at high enough temperatures, self-diffusion parallel to the basal plane should occur by an interstitial mechanism because the migration energy of the interstitial is much lower.

### I. INTRODUCTION

The behavior of point defects in graphite is of great relevance for the study of radiation damage and irradiation effects.<sup>1,2</sup> The determination of the mechanisms for atomic motion in graphite is also important for understanding the high-strength fiber graphitization process. While the structure and energetics of crystalline graphite are fairly well understood, point-defect configurations and self-diffusion mechanisms have not been yet clearly established.

The formation energy of a vacancy,  $Q_v^f$ , estimated from specific-heat data above 3270 K and from thermal conductivity data is 7 eV.<sup>3</sup> On the other hand, assuming that vacancy loop formation by irradiation at 1473 K (Ref. 4) is controlled by single vacancy migration, a value of  $Q_v^{ma} \approx 3$  eV for the in-plane vacancy migration energy has been derived. Loop formation was also observed in quenching and annealing experiments, which gave nearly the same value for  $Q_v^{ma}$  as above but a much lower value of  $Q_v^f$ , viz., 3.3 eV.<sup>5</sup> An estimate of the activation energy required to anneal irradiation-induced interstitial loops gave 5.5 eV. This value has been attributed to the migration energy for vacancy diffusion in the *c*-crystallographic axis direction,  $Q_v^{mc}$ .<sup>5</sup>

The value of activation energy for self-diffusion parallel to the graphite basal plane ("a-axis" diffusion),  $Q_{sd}^a$ , is  $7.1 \pm 0.5$  eV, as determined from radiotracer ( $C^{14}$ ) diffusion in the temperature range from 2000 to 3200 K.<sup>6,7</sup> No direct determination of  $Q_{sd}^c$ , the activation energy for self-diffusion in a direction parallel to the *c*-crystallographic axis ("c-axis" diffusion), has been made. However, the activation energies for boron diffusion in graphite parallel and perpendicular to the basal plane,  $Q_{Bd}^a$  and  $Q_{Bd}^c$ , are the same within experimental scatter (6.8 and 6.6 eV, respectively).<sup>8</sup> Because boron is the only substitutional impurity in graphite, the near coincidence of the values of  $Q_{sd}^a$  and  $Q_{Bd}^a$  led Thrower and Mayer<sup>8</sup> to propose that  $Q_{sd}^a$  is almost isotropic in graphite. Considering that  $Q_{sd}^a = Q_d^f + Q_d^m$  for a diffusion mechanism mediated by defect "d," where  $Q_d^f$  and  $Q_d^m$  are formation and migration energies of the defect "d," respectively, an in-

spection of the pertinent values for the vacancy shows poor agreement for *a*-axis diffusion unless the values estimated from loop formation experiments<sup>5</sup> are used. However, there are many uncertainties involved in deriving the vacancy formation and migration energies. Theoretical calculations may help elucidate point-defect energetics and diffusion mechanism.

For interstitials, the derivation of migration and formation energies is naturally related to the study of radiation damage. The formation energy has been derived considering that the total stored energy at low temperatures is due to the presence of Frenkel pairs (i.e., well-separated vacancy-interstitial pairs).<sup>1,2</sup> A value of  $Q_f^f = 14$  eV for the formation energy of a Frenkel pair<sup>9</sup> gives a minimum value of 7 eV for the formation energy of an interstitial. Migration energy values,  $Q_i^{ma}$ , between 0.02 and 0.2 eV for the interstitial migrating parallel to the basal plane have been deduced from electrical resistance measurements on post-irradiation annealing,<sup>10</sup> radiation-induced dimensional changes,<sup>11</sup> stored energy measurements,<sup>9</sup> and loop nucleation studies.<sup>8</sup>

In addition to the defect mechanisms mentioned above for self-diffusion, it has also been speculated that self-diffusion in graphite could be dominated by a nondefect mechanism (e.g., exchange of two adjacent atoms in a graphite layer).<sup>12</sup>

On the theoretical side, early empirical models hardly give accurate descriptions on covalent bonding of carbon atoms (e.g., three-coordinated  $sp^2$  bonding in graphite), and hence calculation results are associated with uncertainties. Recently, Kaxiras and Pandey<sup>12</sup> studied the in-plane diffusion in graphite by performing first-principles calculations with a two-dimensional supercell geometry in the local-density functional approximation (LDA). They obtained that the lowest saddle-point energy corresponds to a vacancy diffusion mechanism.

A general analysis of self-diffusion in graphite that also encompasses diffusion parallel to the *c* axis has never been quantitatively attempted. In this paper, we present calculations on point-defect energetics in graphite using a tight-binding (TB) interatomic potential for carbon developed recently.<sup>13</sup> Several possible diffusion mechanisms, both in-plane and out-of-plane, are investigated.

## II. THEORETICAL MODEL AND METHOD

In the TB scheme used here,<sup>13</sup> the total energy of the system,  $E_{\text{tot}}$ , combines an electronic structure bonding term and a classical repulsive potential energy term. The bonding term is obtained by summing single-electron energies over all occupied electronic states, which are determined by a set of tight-binding parameters. The variations of these parameters with interatomic separation  $r$  are described by smooth short-ranged functions. The repulsive potential energy term is expressed as

$$\sum_i f \left[ \sum_j \phi(r_{ij}) \right],$$

where  $\phi(r_{ij})$  is a pair-wise interaction potential between atoms  $i$  and  $j$ , and  $f$  is a functional of the sum of  $\phi(r_{ij})$  over all atoms other than  $i$ . The parameters of this TB total energy model are obtained by fitting  $E_{\text{tot}}(r)$  to the results of first-principles LDA calculations for the low-energy crystalline phases of carbon in the diamond, graphite, and linear chain structures.

This model describes well the energy versus volume relations for graphite, diamond, and a linear-infinite carbon chain. Dynamic properties such as the phonon spectra and the in-plane elastic constants of graphite are also adequately predicted. However, the calculated shear elastic constants for diamond are too soft.<sup>13</sup> Calculations of the ground-state geometries of carbon clusters in the range of  $C_2$  to  $C_{10}$  yield results which are in very good agreement with corresponding results from quantum chemical calculations. Investigations on some properties of liquid carbon using this model give excellent agreement with *ab initio* Car-Parrinello calculations. These results<sup>13,14</sup> demonstrate that the potential has good transferability to a wide variety of bonding environments involving coordinations of two, three, and four atoms thus conferring reliability to the calculations of energetics and properties on defect systems such as point defects in graphite.

The TB potential has a cutoff distance of 2.6 Å, which is larger than the in-plane lattice constant ( $a_0$ ) of 1.42 Å but smaller than the interlayer distance of 3.35 Å. For a graphite layer in equilibrium, direct atomic interactions up to second nearest neighbors can be taken into account. Our interest focused on in-plane as well as out-of-plane defects. Although the range of the potential precludes describing the weak interlayer interaction directly, it allows us to study out-of-plane defects such as the interstitial provided its distance to a lattice atom is within the range of the potential.

In this investigation, the TB scheme<sup>15</sup> is applied to study the in-plane defects by a two-dimensional supercell and the out-of-plane defects by a three-dimensional supercell (i.e., fully periodic boundary conditions are used in both cases). The volume of the unit cell is kept constant. The two-dimensional unit cell (of a rectangular shape) consisting of 112 atoms is used in most of the calculations. The dimensions of the rectangular shape cell are  $12a_0$  by  $7\sqrt{3}a_0$ . For describing interplane interstitials, the unit cell consists of two layers of 224 atoms. Convergence tests are performed by calculating the energy of a single vacancy using 2D cells of 60, 112, and 240

atoms (which have formation energies of 8.1, 7.5, and 7.3 eV, respectively), and by calculating the energy of an interstitial with unit cells of two and four layers. An inspection of these results shows that the choices of a 2D unit cell of 112 atoms for in-plane defects and a two-layer unit cell of 224 atoms for interstitials give reasonable descriptions for most cases.

## III. IN-PLANE DEFECTS AND DIFFUSION MECHANISM

Possible atomic diffusion mechanisms in graphite can be divided into two categories: nondefect mechanism (e.g., atomic migration through atom pair exchange), and defect mechanism (mediated by vacancies or interstitials). First, we consider the nondefect mechanism. The atom pair exchange involves only one activation since there is no defect mediation. This energy is generally considered to be large because of the occurrence of large lattice distortion near the direct-exchange atom pair during the atomic migration process. In our calculation, the displacements of the exchanging atoms are given by a rotation of the line joining the exchanging atoms from  $\theta=0$  to  $90^\circ$ , with respect to the original orientation [Fig. 1(a)]. For each  $\theta$  value chosen, the lattice is allowed to relax in the TB force field under the constraint that the exchanging atoms can only change their distance along the line connecting them. Figure 1(b) illustrates the relaxation

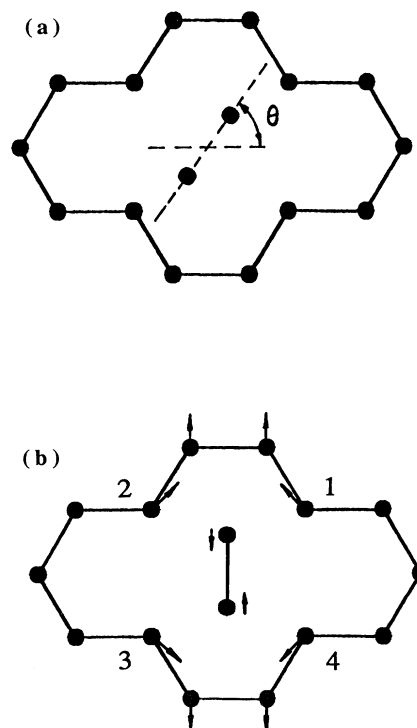


FIG. 1. (a) Intermediate (and unrelaxed) position for the direct exchange of two atoms. These two atoms have been displaced from their initial positions by an angle  $\theta$ , and (b) relaxed lattice configuration corresponding to  $\theta=90^\circ$ , showing the displacement directions of four nearest-neighbor atoms (marked as 1, 2, 3, and 4).

directions of the exchanging pair and of their first- and second-nearest neighbors (the atomic relaxations of lattice atoms are found to confine on the basal plane). The resulting energy change per atom as a function of  $\theta$  is shown in Fig. 2. The overall trend is very similar to the curve predicted by first-principles calculation.<sup>12</sup> Two energy maxima are obtained near  $\theta=50^\circ$  and  $130^\circ$ , fairly close to the values of  $55^\circ$  and  $125^\circ$  observed in Ref. 12. The values of the energy barriers of 9.8 eV and the energy of 5.8 eV at the middle point ( $\theta=90^\circ$ ), however, differ substantially from the corresponding values of 14.0 and 11.4 eV (10.4 eV, for the “relaxed” geometry) from Ref. 12. This discrepancy is not surprising, considering that, in Ref. 12, unrelaxed exchange configurations were used for most of the rotations and a constrained relaxation was adopted in the only configuration ( $\theta=90^\circ$ ) where relaxation was performed (i.e., the relaxation was allowed only along their pairwise connecting lines at  $\theta=55^\circ$  and  $125^\circ$ , respectively, for the four first nearest neighbors of the exchanging pair). We find from our result of exchanging atoms at  $\theta=90^\circ$  that the displacements of the four nearest neighbors are along  $\theta=129^\circ$  and  $51^\circ$ , respectively [Fig. 1(b)], quite different from the inward relaxation pattern involving four nearest-neighbor atoms in Ref. 12. An inspection of the relaxed geometry reveals that the displacements of atoms up to fifth nearest neighbors are very significant, with 18%  $a_0$  in both the first and the second nearest neighbors, and still as high as 12%  $a_0$  in the fifth neighbors. These results indicate that simulations limiting the relaxations to first nearest-neighbor atoms alone in a constrained supercell geometry might be inadequate. In fact, the energy versus  $\theta$  relation for the unrelaxed exchange configuration obtained in our calculation is already substantially different from that obtained in Ref. 12. The relaxation for  $\theta=50^\circ$  and  $\theta=90^\circ$  actually reduces the energies by 6.6 and 11.9 eV, respectively. These large relaxation energies are due to the large compression or stretching of bonds near the exchanging atoms. If exchange were a plausible diffusion mechanism,

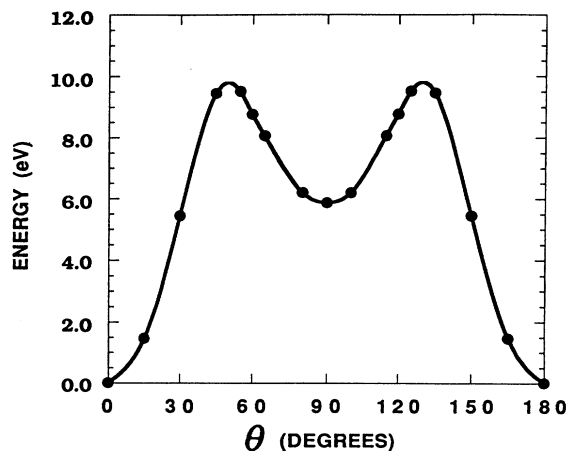


FIG. 2. Energy change per atom versus rotation angle for activating the exchange process associated with the in-plane exchange mechanism. The maxima of the energy barrier occur at  $\theta=50^\circ$  and  $130^\circ$ .

the pertinent path is likely to exhibit a single maximum which corresponds to the saddle-point configuration (i.e.,  $\theta=90^\circ$ ).<sup>16</sup> It has thus been conjectured that exchange of two atoms might occur along an out-of-plane path and be associated with a lower activation energy than the double barriers. We have therefore performed calculation for an out-of-plane rotation similar to the in-plane one, except that the rotation plane is normal to the basal plane. An energy barrier of 14.0 eV is obtained for activating this exchange process showing that this path is not plausible. The atomic relaxations in this case are mostly perpendicular to the basal plane. We have also examined a case in which the rotation plane makes an angle 35 degrees with the basal plane, i.e., a situation in between the two cases considered above. The overall trend of the energy change as a function of  $\theta$  for activating this exchange process is very similar to that of the in-plane rotation (i.e., a double-barrier curve depicted in Fig. 2). We obtain energy barriers of about 10 eV and an energy value of 6.0 eV at  $\theta=90^\circ$  for the present case.

We consider next the vacancy-mediated self-diffusion parallel to the basal plane. The vacancy configuration and the directions of calculated atomic relaxations are indicated in Fig. 3(a). From symmetry considerations, the saddle point for atomic migration is considered as the split-vacancy configuration [Fig. 3(b)]. We obtain for the relaxed geometries a formation energy  $Q_v^f$  of 7.3 eV and a migration energy  $Q_v^m$  of 1.0 eV. The value of  $Q_v^f$  calculat-

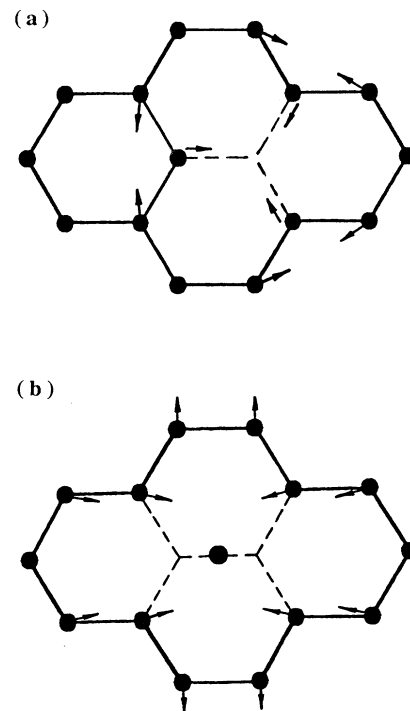


FIG. 3. (a) Atomic relaxation pattern of a single vacancy configuration. Arrows indicate relaxation directions for the first and second nearest neighbors of a vacancy, and (b) atomic relaxation pattern of a split-vacancy configuration.

ed here agrees fairly well with the value of 7.8 eV (which does not include relaxation energy) reported in Ref. 12. It is likely that a better agreement should be expected if relaxation effect and a larger supercell could be used in the LDA calculation. (Our convergence test on the unit cell size shows that the use of a smaller cell tends to increase the value of  $Q_v^f$ .) We find that in the relaxed configuration, the vacancy's first and second neighbors are displaced about 2% of the interatomic distance  $a_0$  and the relaxation energy is 0.11 eV. The displacement of the third and further neighbor atoms is, however, much smaller (less than 1% of  $a_0$ ). The calculated vacancy formation energy is in excellent agreement with the higher value estimated from experiment.<sup>6,7</sup> The value of 1 eV calculated here for  $Q_v^{ma}$  is substantially lower than the value estimated from experiment, although the activation energy for self-diffusion (i.e.,  $7.3 \pm 1.0 = 8.3$  eV) would be in fair agreement with the results from tracer experiments ( $7.1 \pm 0.5$  eV).<sup>6,7</sup> LDA calculations of Ref. 12 have also obtained a low "unrelaxed" value of  $Q_v^{ma}$ , 1.9 eV. Again we think that the difference with our calculation is caused largely by the absence of lattice relaxation in their study. In fact, we find that the lattice relaxations for the case of split vacancy is substantial (10%  $a_0$  for the first nearest neighbors, 1.4%  $a_0$  for the second, 8%  $a_0$  for the third, and less than 4%  $a_0$  for the farther neighbor atoms), and a large relaxation energy (1.6 eV) is obtained. This kind of oscillatory displacement pattern in the relaxation was also obtained in a study of point defects in crystalline silicon.<sup>17</sup> The activation energy for self-diffusion in the basal plane mediated by vacancies ( $Q_{sd}^a = 8.3$  eV) is lower than the activation energy of atom pair exchange ( $= 9.8$  eV). Our calculation thus rules out a nondefect mechanism for self-diffusion in graphite.

Di-vacancies have a formation energy of 9.5 eV which corresponds to a large binding energy, 5.1 eV. This implies a strong tendency of vacancies to aggregate at temperatures where they become mobile.

#### IV. INTERSTITIAL DIFFUSION PARALLEL TO THE BASAL PLANE

An accurate theoretical evaluation of the formation and the  $a$ -axis migration energies of interstitials is required not only to the understanding of atomic motion but to the study of radiation damage. Based on the available experimental data, Thrower and Mayer<sup>8</sup> suggested that the values of  $Q_i^f$  and  $Q_i^{ma}$  are 7.0 eV and less than 0.1 eV, respectively.

In the present study, interstitials are placed at several different sites between graphite layers (Fig. 4), and calculations are performed for each configuration allowing all atoms to relax until an energy minimum is attained. The values of  $Q_i^f$  at sites  $A$ ,  $B$ ,  $C$ , and  $E$  are close to 7.1 eV (to within 0.03 eV), which is in very close agreement with the value suggested from experiment.<sup>8</sup> The value of  $Q_i^f$  at site  $D$  (where the interstitial has atoms directly above and below), however, is higher with a value of 7.7 eV. Thus, if site  $D$  were a saddle-point configuration, the energy barrier  $E_i^{ma}$  would be 0.6 eV. This leads us to suggest that an interstitial is more likely to form at sites  $A$ ,  $B$ ,

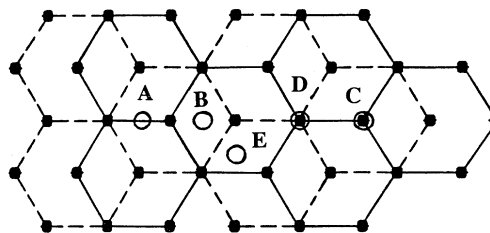


FIG. 4. Possible interstitial sites (labeled by  $A$ ,  $B$ ,  $C$ ,  $D$ , and  $E$ ) between basal planes. Solid and dashed lines represent upper and lower basal planes, respectively.

and  $C$  than at site  $D$ , and as it moves parallel to the basal plane, it should detour from the energy islands located at  $D$  sites and migrate via other routes (for example, via  $E$  site) relating to lower activation energies (i.e., less than 0.03 eV).

#### V. SELF-DIFFUSION ALONG THE $c$ -AXIS DIRECTION

As described in the Introduction, it was suggested that the activation energy in graphite is almost isotropic in spite of the high crystallographic anisotropy.<sup>8</sup> Thrower and Mayer speculated that if Frenkel pairs could exist in equilibrium, the interstitial, being the fast diffusing species, could account for diffusion parallel to the  $c$  axis. Therefore, they analyzed possible interstitial diffusion mechanisms to account for this isotropy. Theoretical investigation to test the possibility of diffusion along the  $c$  axis have been challenging since the conjectured mechanisms are likely to be associated with long-range lattice distortion (and new bonds formation) which often involves lattice relaxations of a large number of atoms. Thus, accurate estimations of the energetics for these mechanisms become difficult in many instances.

We have investigated the following processes as possible means of  $c$ -axis diffusion: (a) penetration of interstitials through graphite layers, (b) vacancy migration between layers, (c) direct exchange of two atoms in adjacent layers, and (d) bonded interstitial and/or interstitialcy mechanism.

For an interstitial penetrating a graphite layer, the saddle point corresponds to locating the interstitial atom at the center of a hexagon. Since the atoms in graphite layer have a tendency to maintain their  $sp^2$ -type bonding, the penetrating interstitial is found to induce a large distortion of the surrounding hexagons in this case. Our calculation gives a migration energy for the interstitial of 3.9 eV for this mechanism. The corresponding activation energy of an interstitial in this configuration is 11.0 eV.

We next consider the activation state for the migration of a vacancy between two adjacent basal planes. The saddle point for vacancy-mediated migration along the  $c$  axis is a split vacancy configuration, i.e., an interstitial atom is placed at site  $D$  between two adjacent layers in Fig. 4, but with the removal of lattice atoms directly above and below. The activation atom in the present calculation is confined in the position midway between two layers in the whole simulation process. The relaxed geometry re-

veals large displacement of atoms near the activated atom, showing that the atoms in the nearby layers tend to bond with the activated atom. We observe the displacements of neighboring atoms in the direction toward the activated atom by distances of 44%  $a_0$  for the nearest neighbors, 23%  $a_0$  for the second, 19%  $a_0$  for the third (and less than 6%  $a_0$  displacement for the farther neighbors). This results in an activation energy of 12.0 eV, or a migration energy of 4.7 eV, making vacancy diffusion between layers a very unlikely mechanism for  $c$ -axis diffusion.

The direct exchange of two atoms in two adjacent layers in the present study is described as rotating the atom pair around the midpoint between two layers as shown in Fig. 5. This displaced atom pair is arranged in the  $xz$  plane along a line making a rotation angle  $\theta$  with the  $z$  axis, and then allowed to relax in the TB force field but constrained to a conical surface of aperture  $\theta$  centered at the rotation point. Calculations are performed for given angles of 45°, 60°, and 90°. A plot of the activation energy versus  $\theta$  yields that an activation energy as high as 11.0 eV is required for this exchange mechanism.

The bonded-interstitial mechanism was argued early by Thrower and Mayer as a possible means of  $c$ -axis diffusion at high temperatures, under the assumption that the interstitial configuration is that shown in Fig. 6 and that the interstitial atom  $I$  forms strong tetrahedral bonds with the atoms marked  $A_1$ ,  $A_2$ ,  $A_3$ , and  $A_4$  in the same figure. The effect of the tetrahedral bonds is further assumed to induce a large distortion of surrounding lattice, which facilitates the interstitial atom to move in the  $c$ -axis direction through the upper atomic plane (see Fig. 6). However, formation of such short bond is not apparent from our calculations. As mentioned earlier, the graphite atoms tend to maintain their  $sp^2$ -type bonding. In fact, the introduction of the interstitial has the effect of displacing neighboring graphite atoms away from the interstitial demonstrating the prevalence of  $sp^2$  bonding.

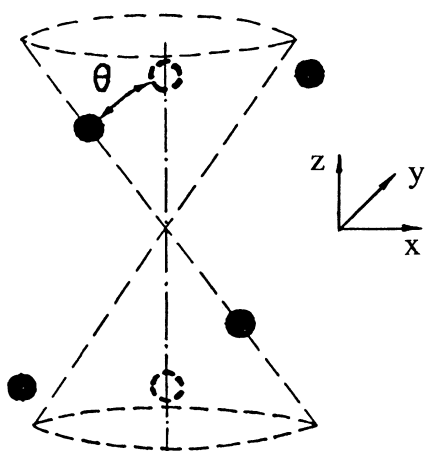


FIG. 5. Atomic configuration for the direct exchange of atom pair between two adjacent layers. The exchanging atoms are rotated from their initial positions (i.e., open circles) by an angle  $\theta$ . See text for details.

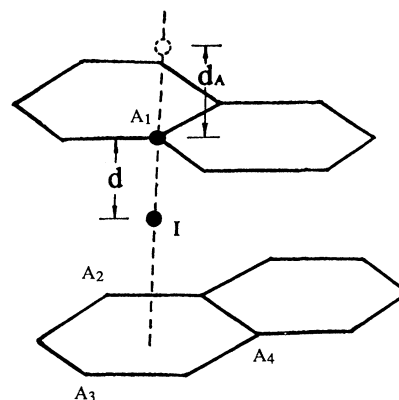


FIG. 6. Atomic configuration for the bonded-interstitial mechanism. The interstitial  $I$  is placed at a distance  $d$  from the upper plane.  $d_A$  is the distance between the "ejected" atom  $A_1$  (dashed circle) and the upper plane.

An inspection of the atomic displacements caused by the presence of the interstitial shows that the interatomic distances between the interstitial and its seven nearest neighbors tend to become equal and that the outward displacement (i.e., away from the interstitial) does not depend on the particular neighbor atom.

We calculate the migration energy of an interstitial in the  $c$ -axis direction via an interstitialcy mechanism (i.e., an interstitial ejects and replaces a lattice atom at the lattice site) as follows. In Fig. 6, interstitial  $I$  is placed at distance  $d$  from a basal plane in which atom  $A_1$  is expected to be knocked out of the plane to become a new interstitial as atom  $I$  approaches. The atom  $I$  is constrained at its place of insertion while all the other atoms are allowed to relax. The calculated energies versus distance  $d$  are plotted in Fig. 7. The migration energy barrier that atom

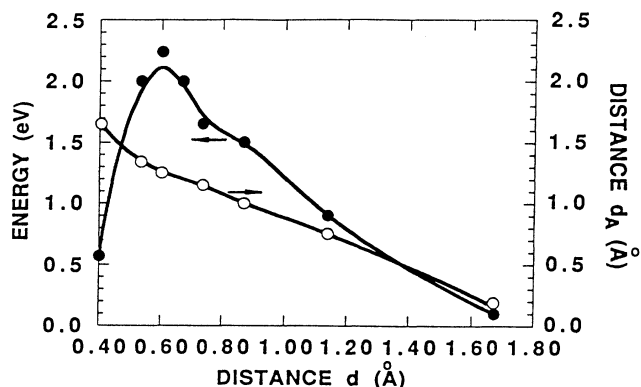


FIG. 7. Migration energy barrier of an interstitial migrate along the  $c$  axis for bonded-interstitial mechanism. The interstitial is placed initially at a distance  $d = 1.675$  Å (i.e., midpoint between two basal planes) from the upper plane (see Fig. 6). The reference point for the energy is taken as the formation energy of an interstitial at site  $C$  in Fig. 4. The corresponding distance  $d_A$  for the "ejected" atoms as a function of  $d$  is shown as open circles.

I should overcome is near 2.3 eV, showing that the interstitialcy mechanism is more probable than the other three mechanisms for  $c$ -axis diffusion. Also plotted in Fig. 7 is the distance between the ejected atom  $A_1$  and the lattice plane ( $d_A$ ) as a function of  $d$ . We observe that the process of atom  $A_1$  breaking bonds with the neighboring atoms in the basal plane and jumping into another interstitial site is closely related to the process of atom I overcoming the migration barrier of 2.3 eV. However, considering that the activation energy for self-diffusion of an interstitial via the interstitialcy mechanism is given by

$$Q_{sd}^c = \frac{1}{2}(Q_v^f + Q_i^f) + Q_i^{mc} = 9.5 \text{ eV},$$

the value is still too high compared to the calculated activation energy for self-diffusion parallel to the basal plane (i.e.,  $Q_{sd}^a = 8.3 \text{ eV}$ ) and the reported activation energy for  $c$ -axis diffusion of boron (i.e.,  $Q_{Bd}^c = 6.8 \text{ eV}$ ). Within the context of the TB model and possible self-diffusion mechanisms considered here, we do not find any evidence that the activation energy for self-diffusion in graphite is isotropic.

## VI. DISCUSSION AND CONCLUSIONS

The above calculations of energies for in-plane and out-of-plane defects are summarized in Table I. Our calculation provides some relevant information concerning self-diffusion mechanisms in graphite. The formation energies of defects are high, whether it is a vacancy or an interstitial. Perhaps the most interesting result is that the two energies do not differ appreciably and that, hence, it is not unlikely that at high temperatures an equilibrium concentration of Frenkel pairs should exist, provided the formation entropies are comparable as well. That the formation energy of vacancies is high is amply demonstrated by the extremely high temperature required to quench in vacancies, on the order of 3300 K for a concentration of  $\sim 1 \times 10^{-10}$ .<sup>18</sup> If Frenkel pairs are produced, a large recombination might occur during quenching favored by the very high interstitial diffusivity leaving only the small vacancy population detected. Interstitials, in turn, can be introduced by vigorous grinding.<sup>19</sup>

The value of activation energy for vacancy migration can account for self-diffusion parallel to the basal plane, but the value estimated from intrinsic loop formation kinetics is larger than the calculated one. New determinations of  $Q_{sd}$  could shed some light concerning this discrepancy. If Frenkel pairs are equilibrium defects, on the other hand, an interstitial mechanism is likely to be responsible for diffusion. There is little doubt from experimental data on irradiation effects in graphite, as well as the present theoretical calculations, that the interstitial is a fast moving species.

TABLE I. Formation, migration, and activation energies (in eV) for defect and nondefect diffusion mechanisms along the  $a$  and  $c$  axis.

	Mechanism	$E^f$	$E^m$	$E^{\text{act}}$
$a$ -axis diffusion	exchange atom			9.8
	pair			
	vacancy	7.3	1.0	8.3
	interstitial	7.1	$\leq 0.03$	7.2 <sup>a</sup>
$c$ -axis diffusion	exchange atom			11.0
	pair			
	vacancy	7.3	4.7	12.0
	Interstitial (through graphite layer) <sup>b</sup>	7.1	3.9	11.0
	interstitialcy	7.1	2.3	9.5 <sup>a</sup>

<sup>a</sup>Related to Frenkel pair formation and self-diffusion mediated by interstitials.

<sup>b</sup>Penetrating through the center of a hexagon.

The TB force model does not yield any preferential bonding of an interstitial atom located at its energy minimum. In fact, there are several energetically equivalent minima for the interstitial. This is unlikely to be a limitation of the potential which, as mentioned in the Introduction, has been shown to be transferable.<sup>13,14</sup> It is possible that if the constant volume constraint is lifted these equivalent minima will differ slightly in energy. It is thus logical to suggest that interstitial migration has a low activation energy. Thus, the migration path avoids the high-energy sites which would place the diffusing atom in close distance to two atoms at neighboring layer planes. We cannot account, within the present model, for an isotropic self-diffusion activation energy. None of the obvious possibilities involving single defects yields low enough activation energies for both  $a$ - and  $c$ -axis directions. Considering that experimental data relates to high temperatures, other mechanisms involving more complex defects might be operational. It is also worth recalling that the interplane exchange mechanism as studied here yields too large an activation energy to account for  $c$ -axis diffusion. Our calculations rule out the operation of a nondefect mechanism for self-diffusion in graphite.

## ACKNOWLEDGMENTS

This research was sponsored by the Division of Materials Science and the Office of Fusion Energy, U.S. Department of Energy, under contract DE-AC05-84OR21400 with Martin Marietta Energy Systems, Inc.

<sup>1</sup>B. T. Kelly, *Physics of Graphite* (Applied Science, London, 1981).

<sup>2</sup>J. H. W. Simmons, *Radiation Damage in Graphite* (Pergamon, Oxford, 1965).

<sup>3</sup>B. T. Kelly and R. Taylor, in *Chemistry and Physics of Carbon*,

edited by P. L. Walker, Jr. and P. A. Thrower (Marcel Dekker, New York, 1973), Vol. 10, p. 1.

<sup>4</sup>P. A. Thrower, *Carbon* **6**, 687 (1968).

<sup>5</sup>C. Baker and A. Kelly, *Nature* **193**, 235 (1962).

<sup>6</sup>M. A. Kanter, *Phys. Rev.* **107**, 655 (1957).

- <sup>7</sup>R. B. Evans, III, L. D. Love, and E. H. Kobisk, *J. Appl. Phys.* **40**, 3058 (1969).
- <sup>8</sup>P. A. Throter and R. M. Mayer, *Phys. Status Solidi A* **47**, 11 (1978).
- <sup>9</sup>L. Bochirol and E. Bonjour, *Carbon* **6**, 661 (1968).
- <sup>10</sup>C. E. Klabunde, T. H. Blewitt, and R. R. Coltman, *Bull. APS* **6**, 129 (1961).
- <sup>11</sup>D. G. Schweitzer, *Phys. Rev.* **128**, 556 (1962).
- <sup>12</sup>E. Kaxiras and K. C. Pandey, *Phys. Rev. Lett.* **61**, 2693 (1988).
- <sup>13</sup>C. H. Xu, C. Z. Wang, C. T. Chan, and K. M. Ho, *J. Phys.: Condens. Matter* **4**, 6047 (1992).
- <sup>14</sup>C. H. Xu, Ph.D. thesis, Iowa State University (1991).
- <sup>15</sup>C. Z. Wang, C. T. Chan, and K. M. Ho, *Phys. Rev. B* **39**, 8586 (1989).
- <sup>16</sup>If the exchange mechanism is a pertinent mechanism, the exchange atom pair may be trapped in the potential well corresponding to the position of  $\theta=90^\circ$ . However, this type of structure has never been observed experimentally.
- <sup>17</sup>C. Z. Wang, C. T. Chan, and K. M. Ho, *Phys. Rev. Lett.* **66**, 189 (1991).
- <sup>18</sup>G. R. Hennig, *J. Chem. Phys.* **40**, 2877 (1964).
- <sup>19</sup>J. Latcher and R. H. Bragg, *Phys. Rev. B* **33**, 8903 (1986).